



Umbrella-shaped graphene/Si for multi-band tunable terahertz absorber

Jiu-sheng Li¹ · Jian-zhong Sun¹

Received: 12 May 2019 / Accepted: 23 August 2019 / Published online: 31 August 2019
© Springer-Verlag GmbH Germany, part of Springer Nature 2019

Abstract

We demonstrated a triple-band terahertz wave absorber, which consists of umbrella-shaped graphene metasurface array and a gold ground plane separated by a high-resistivity dielectric layer. Simulated results show that the proposed absorber has three distinctive absorption peaks at frequencies 0.506 THz, 1.638 THz, and 2.687 THz with the absorption rates of 0.998, 0.997, and 0.998, respectively. The terahertz absorber is valid to attain $0^\circ \sim 60^\circ$ range of incident angles for both transverse electric (TE) and transverse magnetic (TM) polarizations. For the graphene-based metasurface structures, the absorption curves can be tuned by controlling applied bias voltage. It is a promising candidate to design a high-performance absorber having the potential applications in bolometer, spectroscopic imaging, thermal detector, etc.

1 Introduction

Metamaterial-based terahertz wave absorbers may have promising potential areas such as bolometer, detector, and spectroscopic imaging because of their high performance and compact size [1–4]. However, once these devices are fabricated, their performance cannot be adjusted except for reconstructing the device geometric structures. It is unfavorable for many potential applications. Recently, graphene-based terahertz devices have attracted considerable interest because of their tenability [5–8]. Although with high absorptivity, most of the existing graphene terahertz absorbers are single band, polarization sensitive, and narrow-incident-angle response, which limits their potential applications in bolometer, spectroscopic imaging detection, thermal detector, etc. [9–13]. Polarization insensitive, multi-band, and wide-incident-angle response terahertz wave absorbers are urgently desired. Here we report the multi-band graphene-based absorber using umbrella-shaped graphene metasurface array. The absorber exhibits three frequencies distinctive absorption peaks with near unity absorptivity for both TE and TM polarizations. Moreover, the presented graphene-based terahertz absorber has polarization insensitivity, and a wide operating incident angle with more than

0.995 absorption rate is up to 60° . These charming features make it a good candidate for potential applications such as bolometer, spectroscopic imaging, thermal detector, etc.

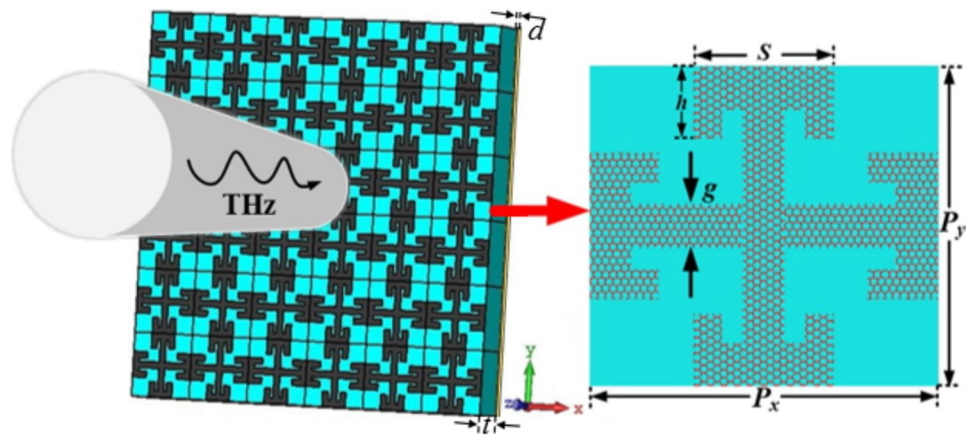
2 Terahertz absorber design and analysis

Figure 1 shows schematic of the multi-band terahertz wave absorber as well as the propagation configurations of the incident terahertz wave. The proposed graphene-based absorber is made up of three layers. The top layer consists of an array of umbrella-shaped graphene metasurfaces, which is responsible for electric response to the incident terahertz wave. The bottom metallic layer is a gold plane with a conductivity of $\sigma = 4.56 \times 10^7 \text{ S/m}$ and a thickness of $d = 1 \mu\text{m}$ exciting anti-parallel surface current to the top layer, which is responsible for the magnetic response. By using the commercial program CST Microwave StudioTM 2018, we performed computer optimization of the proposed terahertz wave absorber and obtained the optimized structure parameters as follows: $p_x = p_y = 50 \mu\text{m}$, $t = 41 \mu\text{m}$, $g = 5 \mu\text{m}$, $d = 1 \mu\text{m}$, $s = 20 \mu\text{m}$, and $h = 12 \mu\text{m}$. The dielectric layer is silicon with electric permittivity $\epsilon_r = 11.9$ and loss tangent $\tan\delta = 0.001$. Both x - and y -directions of the unit cell are defined as periodic boundary conditions, and the z -direction is set as open boundary condition for the terahertz wave incidence and transmission. The incident wave was modeled as a Floquet port in z -direction. S_{11} can be simulated by S-parameters from CST Microwave Studio simulation. Due to the gold ground plane, notice that no terahertz wave penetrates

✉ Jiu-sheng Li
jshli@126.com

¹ Centre for THz Research, China Jiliang University,
Hangzhou 310018, China

Fig. 1 Schematic of the proposed terahertz absorber consisting of graphene metasurface and bottom gold film, separated by a silicon spacer. The geometrical parameters of graphene-based metasurface structures are $p_x=p_y=50\ \mu\text{m}$, $t=41\ \mu\text{m}$, $g=5\ \mu\text{m}$, $d=1\ \mu\text{m}$, $s=20\ \mu\text{m}$, $h=12\ \mu\text{m}$, respectively



the structure; therefore, the transmission of the absorber S_{21} is close to 0 (i.e., $T(\omega)=|S_{21}|^2=0$). The absorptivity of the absorber is defined as $A(\omega)=1-R(\omega)-T(\omega)$, where $R(\omega)$ and $T(\omega)$ are the reflectivity and transmissivity as functions of frequency, respectively. Then the absorptivity of the presented terahertz absorber becomes $A(\omega)=1-R(\omega)=1-|S_{11}|^2$. The graphene's surface conductivity can be well described by the Kubo formula as follows [14]

$$\sigma(\omega, \mu_c, \Gamma, T) = \sigma_{\text{intra}} + \sigma_{\text{inter}}, \tag{1}$$

$$\sigma_{\text{intra}} = \frac{je^2}{\pi\hbar^2(\omega - j2\Gamma)} \int_0^\infty \xi \left(\frac{\partial H(\xi, \mu_c, T)}{\partial \xi} - \frac{\partial H(-\xi, \mu_c, T)}{\partial \xi} \right) d\xi, \tag{2}$$

$$\sigma_{\text{inter}} = -\frac{je^2(\omega - j2\Gamma)}{\pi\hbar^2} \int_0^\infty \frac{H(-\xi, \mu_c, T) - H(\xi, \mu_c, T)}{(\omega - j2\Gamma)^2 - 4(\xi/\hbar)^2} d\xi, \tag{3}$$

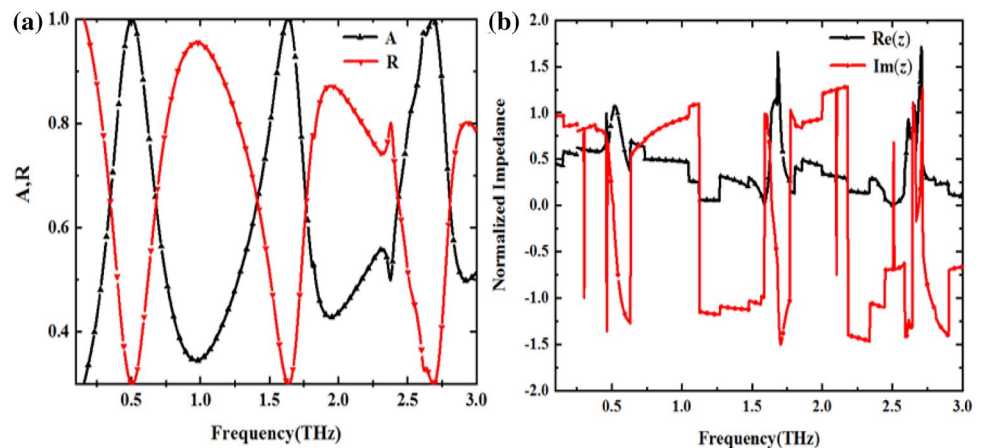
$$H(\xi, \mu_c, T) = \left(e^{(\xi-\mu_c)/k_B T} + 1 \right)^{-1}, \tag{4}$$

where ω is the radian frequency, μ_c the chemical potential, $\Gamma=1/(2\tau)$ the phenomenological scattering rate, τ the electron-phonon relaxation time, T the temperature of Kelvin, σ_{intra} and σ_{inter} the intra-band and inter-band transition, respectively, e the charge of an electron, \hbar the reduced Planck's constant, ξ energy of electrons, $H(\xi, \mu_c, T)$ the Fermi-Dirac distribution, and k_B is the Boltzmann's constant. At room temperature $T=300\ \text{K}$, the Kubo equation is reduced to a Drude-like form, which is:

$$\sigma = \frac{ie^2\mu_c}{\pi\hbar^2(\omega + i\tau^{-1})}. \tag{5}$$

We simulated the absorptivity and reflectivity curves of the proposed umbrella-shaped graphene metasurface absorber with the optimized structure parameters (here, the chemical potential and the relaxation time of graphene metasurface are set as 0.7 eV and 0.1 ps, respectively), as depicted in Fig. 2a. One can clearly see that there are three distinctive high absorption peaks (above 99.5%) at the frequencies of 0.506 THz, 1.638 THz, and 2.687 THz. To achieve perfect absorption, the normalized impedance of

Fig. 2 **a** Absorption and reflection spectra of the absorber **b** real and imaginary parts of the normalized surface impedance of the proposed absorber



the presented absorber should match that of the free space ($Z/Z_0=1$). The effective normalized impedance of our absorber can be described as [15]:

$$z = \sqrt{\frac{(1 + S_{11})^2 - S_{21}^2}{(1 - S_{11})^2 - S_{21}^2}}, \tag{6}$$

where S_{21} and S_{11} denote as transmittance and reflectance coefficient, respectively. The values of these scattering parameters can be obtained by numerical simulation using the CST Microwave Studio. Furthermore, according to Eq. (6), we calculate the effective normalized impedance of the absorber, as shown in Fig. 2b. The effective normalized impedances are $Z=1.05+0.05i$, $Z=1.01-0.03i$, and $Z=1.03+0.01i$ at three resonance frequencies 0.506 THz, 1.638 THz, and 2.687 THz, which are almost the same as the impedance of the free space. This indicates that the designed absorber realizes the impedance matching between the present absorber structure and free space. Obviously, the absorber exhibits complete absorption of the incident terahertz wave at three resonance frequencies.

Figure 3 depicts the electric fields on the top graphene layer at three absorption frequencies. The umbrella-shaped graphene metasurface’s sides that are parallel to the electric component of incident terahertz wave can couple with the electric field and supply electric dipole response, and then the surface charge oscillates along the umbrella-shaped graphene metasurface sides driven by the external

electric field. From Fig. 3c and f, notice that the magnetic response between the top layer and bottom layer at frequency 2.687 THz for 0.3 eV becomes stronger than the magnetic response of other chemical potential. But they are almost the same as the dipole electric response of the top umbrella-shaped graphene metasurfaces under three different chemical potentials. Therefore, there are two peaks at frequency 2.687 THz for 0.3 eV chemical potential instead of one peak for other chemical potential. The surface current distributions on top graphene pattern layer and bottom metallic layer of the terahertz absorber at absorption peaks (i.e., 0.506 THz, 1.638 THz, and 2.687 THz) are displayed in Fig. 4a–f. The magnetic component of the incident terahertz wave penetrates between the top umbrella-shaped graphene metasurface and the bottom metallic layers and generates anti-parallel surface current on the umbrella-shaped graphene metasurfaces and the ground gold plane, leading to the magnetic coupling response. From Figs. 3 and 4, one can notice that the three absorption peaks of the absorber originate from the dipole electric response of the top umbrella-shaped graphene metasurfaces and the magnetic response between the top and bottom layers.

We perform finite element method numerical simulations to investigate the structure parameters influence on the terahertz wave absorber. Figure 5a shows the influence of the chemical potential values on the absorption spectra of the proposed structure. As the graphene chemical potential increases from 0.3 eV to 0.8 eV, the amplitude of the three absorption peaks increases from 94 to 99.8%,

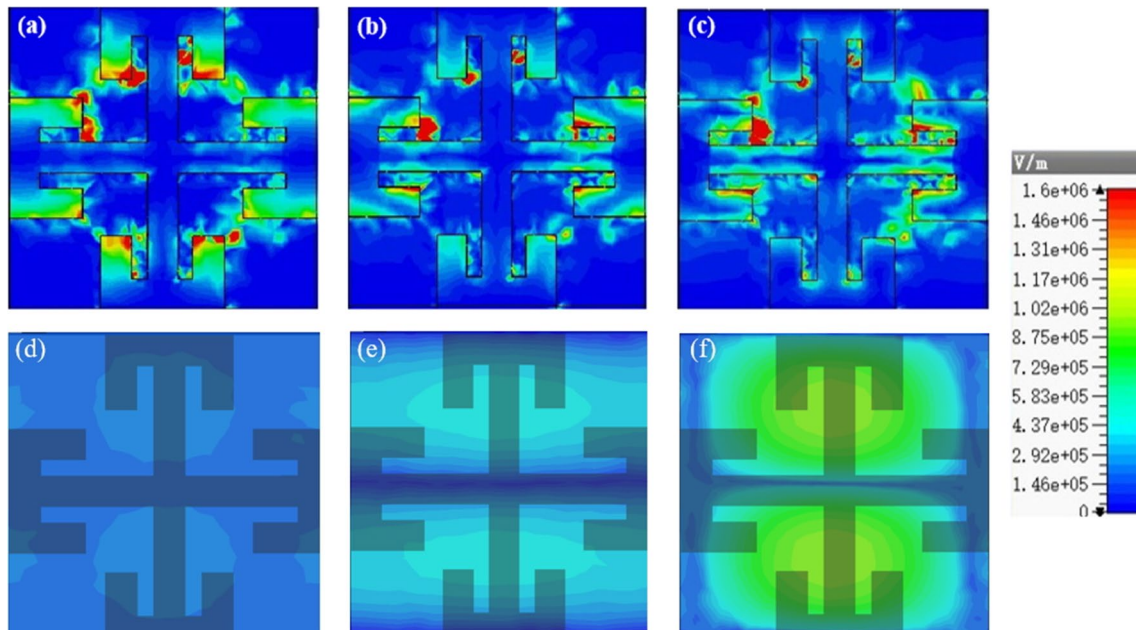


Fig. 3 Electric field distribution on the top layer at the three absorption peaks (a–c) **a** $f_1=0.506$ THz, **b** $f_2=1.638$ THz, **c** $f_3=2.687$ THz, and on the bottom layer (d–f), **d** $f_1=0.506$ THz, **e** $f_2=1.638$ THz, **f** $f_3=2.687$ THz

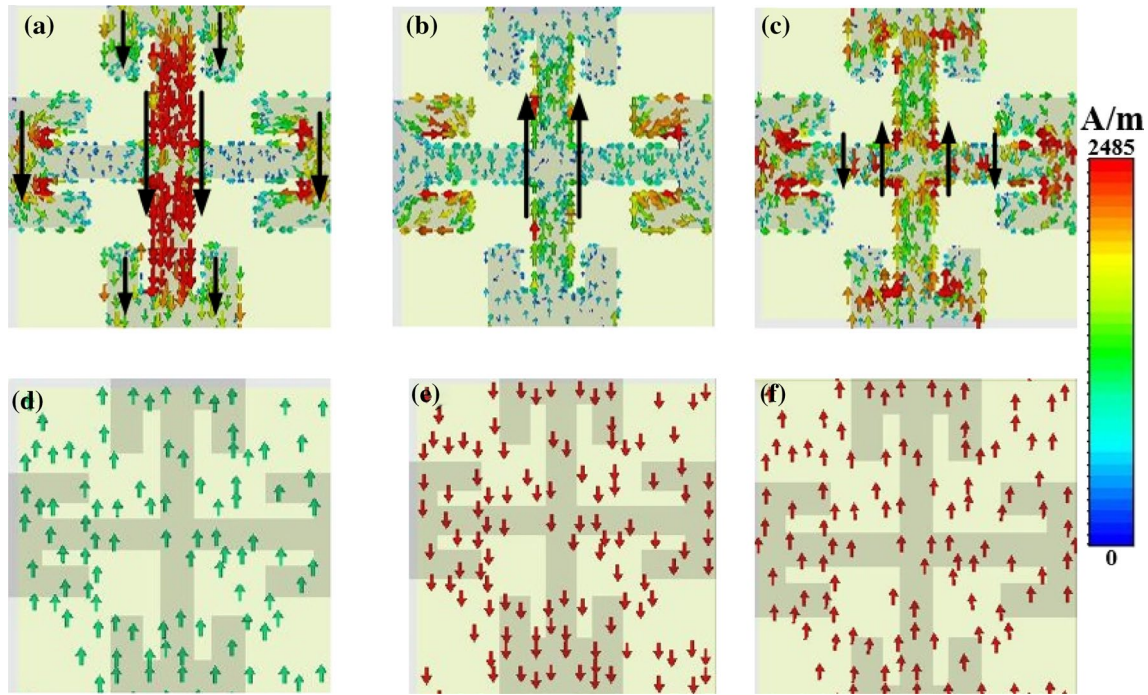


Fig. 4 Surface current distributions on the top layer at the resonance points (a~c), **a** $f_1=0.506$ THz, **b** $f_2=1.638$ THz, **c** $f_3=2.687$ THz, and on the bottom layer (d~f), **d** $f_1=0.506$ THz, **e** $f_2=1.638$ THz, **f**

$f_3=2.687$ THz at x - y plane and $z=0$. (Here, arrows denote for the direction and color denote for the intensity)

and the center frequencies of the absorption peaks have a slight blue shift. It can be observed that the absorptivity and the working center frequencies of the absorber can be effectively adjusted by manipulating the Fermi level of the umbrella-shaped graphene metasurfaces according to the actual applications without redesigning the device structure. As can be seen from Fig. 5b, with the increase in the relaxation time of the graphene metasurface τ from 0.1 ps to 0.3 ps, the absorptivity of the terahertz absorber decreases gradually and three working center frequencies of the absorber appear distinctive blue shift. As the relaxation time of graphene increases, carrier concentration decreases and impedance mismatch occurs. And then the absorptivity of the absorber decreases. Obviously, the relaxation time of the graphene metasurface τ needs to be set at 0.1 ps. Figure 5c shows the frequency behavior of the absorptivity for different silicon thickness of the geometrical parameter t ranging from 36 μm to 46 μm . It is noted that three center frequencies of the absorption peaks have red shifting with the increase in silicon thickness t . But when $t=46$ μm , the second absorption peak exhibits lower than 0.995. Thus, the silicon thickness of parameter t is set as 41 μm . We also calculate the absorption spectra of the absorber when the width of graphene microstrip of the parameter g varies from 4 to 6 μm (see Fig. 5d). It can be noted that the device exhibits three frequencies distinctive absorption peaks with near unity absorptivity

for $g=5$ μm . Therefore, the width of graphene microstrip of the parameter g is fixed as 5 μm .

According to the transmission line theory, the equivalent circuit model of the designed absorber is shown in Fig. 6. The reflectivity of the presented terahertz absorber can be calculated by:

$$R = \frac{\text{Re}\{z_{in}\} - z_0}{\text{Re}\{z_{in}\} + z_0}, \quad (7)$$

where Z_{in} is the input impedance of the transmission line, $1/Z_{in} = 1/Z_1 + 1/Z_g$, Z_0 is the impedance in free space, $Z_0=377$ Ω ; Z_1 is the impedance of intermediate dielectric silicon layer, $z_1 = jZ_t \tan(k_m t)$, $z_t = \omega\mu_0/k_m$, $k_m = \sqrt{k_p^2 - k_0^2 \sin^2 \theta}$, $k_p = \omega\sqrt{\mu_0\epsilon_p}$, where μ_0 is the vacuum permeability, ϵ_p the dielectric constant of silicon, $\epsilon_p=11.9$; Z_g is the surface impedance of the umbrella-shaped graphene metasurface array layer, $z_g = 1/\sigma_g^{\text{eff}}$, σ_g^{eff} is the effective conductivity of graphene pattern structure, $\sigma_g^{\text{eff}} z_0 = (2\sqrt{n_1 n_2} - (n_1 + n_2))/S_{21}$, n_1 and n_2 are the refractive index of the air layer and the intermediate dielectric silicon layer, respectively. Here, S_{21} represents the transmission coefficient of terahertz wave through graphene image layer into intermediate silicon. According to the equation, we can obtain the real and imaginary parts of the surface impedance of the umbrella-shaped graphene metasurface array layer (see Fig. 7a). Figure 7b illustrates the comparison of the

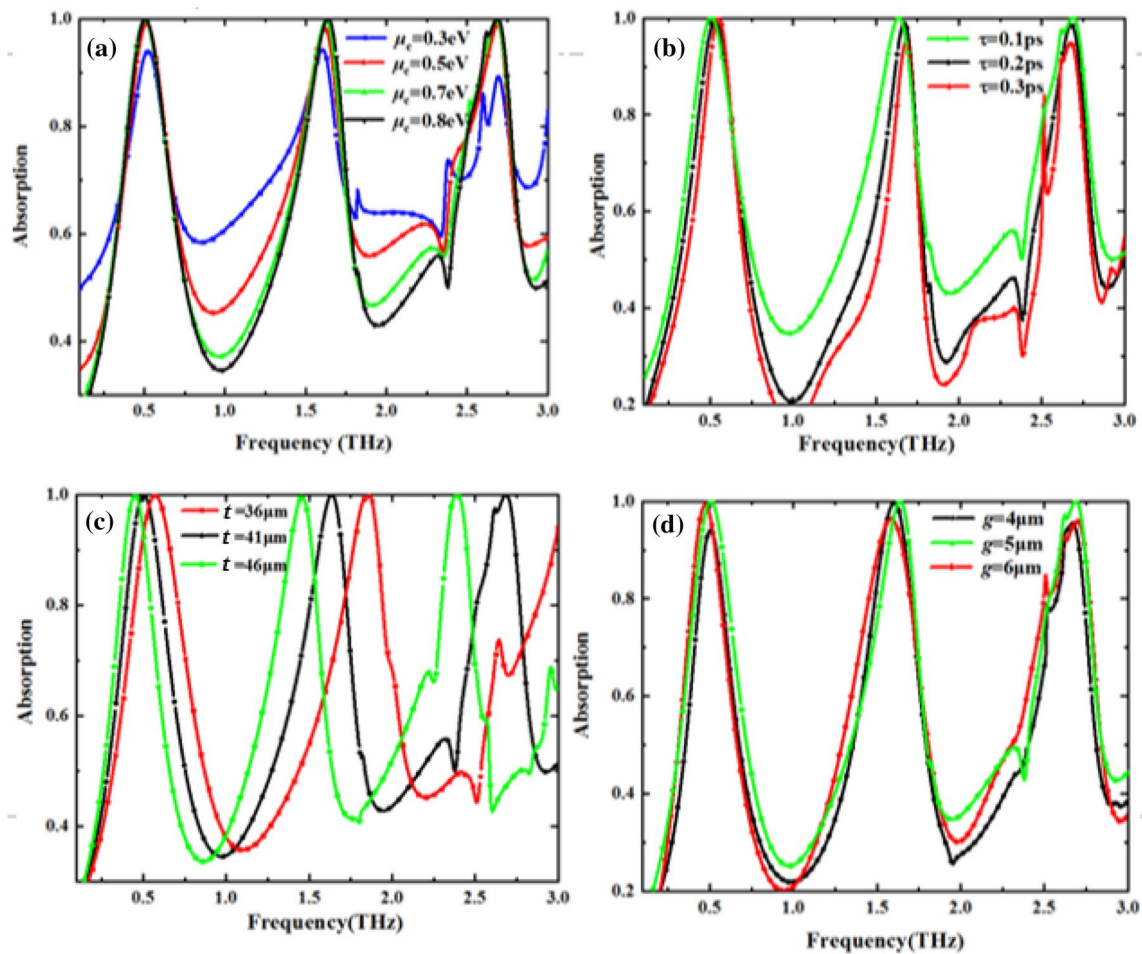


Fig. 5 Absorption characteristics of the terahertz wave absorber for various chemical potential values of μ_c (a), relaxation time values of τ (b), Si thickness values of t (c), and width of graphene microstrip values of g (d)

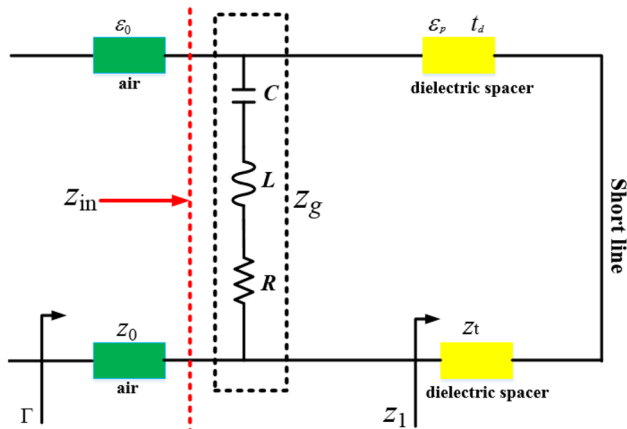


Fig. 6 Equivalent circuit model of the designed absorber

As shown in Fig. 7, the theory calculated (red dot curve) has three absorption peaks at frequencies 0.506 THz, 1.638 THz, and 2.687 THz with absorptivity of 0.998, 0.997, and 0.998, respectively, which agrees well with the simulation results as plotted in Fig. 7 (black curve). Figure 8a and b demonstrates the robustness of the proposed absorber for both TE and TM polarizations under oblique incidence ranging from 0° to 60° , respectively. It can be noted that the prominent triple band, polarization insensitive, and wide incident-angle working capabilities are demonstrated by these figures. From the figure, one sees that three frequencies absorption peaks exhibit near unity absorptivity for both TE and TM polarizations. In addition, it can also be noted that the three center frequencies of the absorption peaks have a slight blue shifting with the increase in incident angle.

absorption spectra of the triple-band graphene metasurface absorber between the transmission line theory calculated (red dot curve) and the CST simulated (black curve) results.

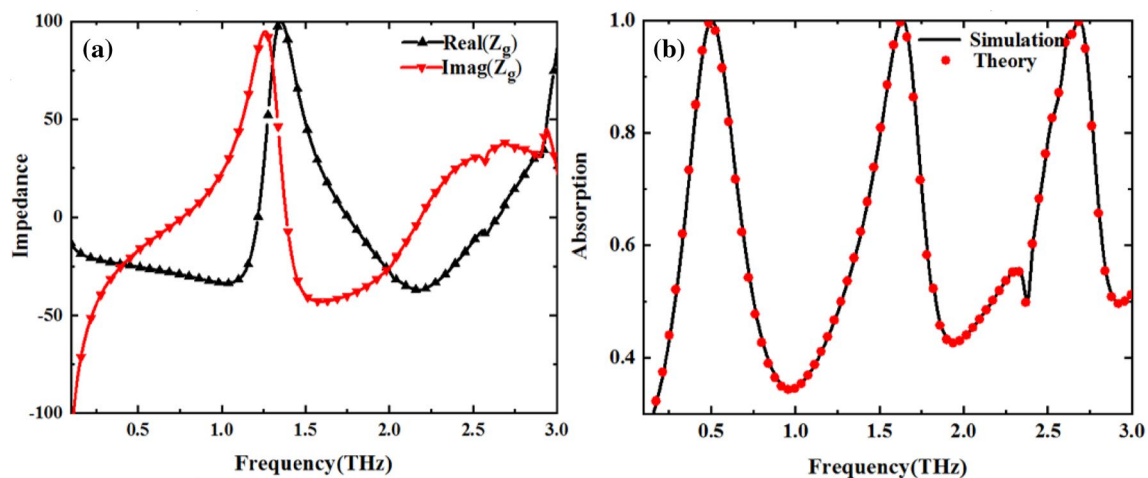
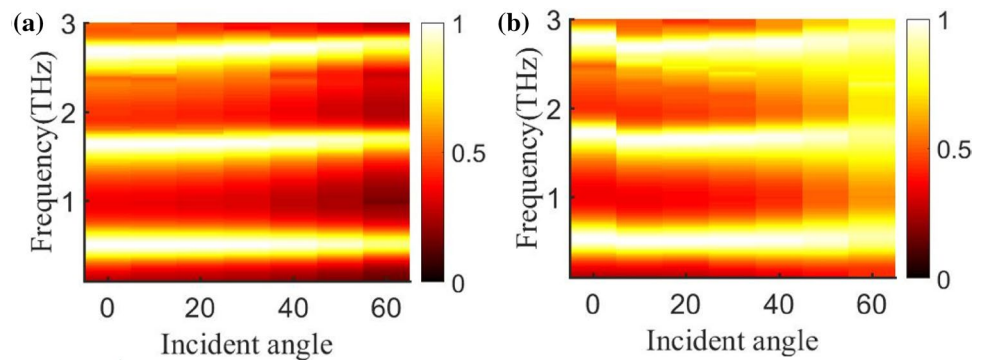


Fig. 7 **a** Real and imaginary parts of the surface impedance of the umbrella-shaped graphene metasurface array layer, **b** comparison of the absorption spectra of the graphene metasurface absorber between

the transmission line theory calculated (red dot curve) and CST simulated (black curve) results

Fig. 8 Absorption spectrum with various incident angles from 0° to 60° of the terahertz absorber for **a** TE- and **b** TM-polarization



3 Conclusion

In conclusion, we have demonstrated a tunable multi-band terahertz wave absorber based on graphene metasurface with three distinctive absorption peaks at three separated frequencies 0.506 THz, 1.638 THz, and 2.687 THz with the absorptivity of 0.998, 0.997, and 0.998, respectively. The results show that the triple absorptions of the designed graphene-based absorber remain near unity absorptivity as the terahertz wave incident angle range from 0° to 60° . Due to the charming features of multiband absorption, wide-angle response, compact size, polarization insensitivity, and adjustability, the terahertz wave absorber is a promising candidate for bolometer, sensors, solar cells, etc.

Acknowledgements We acknowledge financial support from National Natural Science Foundation of China (Grant Nos. 61871355, 61831012), and Zhejiang Province Natural Science Foundation under Grant No. LY18F010016.

References

1. H. Tao, C.M. Bingham, A.C. Strikwerda, D. Pilon, D. Shrekenhamer, N.I. Landy, K. Fan, X. Zhang, W.J. Padilla, R.D. Averitt, Highly flexible wide angle of incidence terahertz metamaterial absorber: design, fabrication, and characterization. *Phys. Rev. B* **78**(24), 241103 (2008)
2. Q.Y. Wen, H.W. Zhang, Y.S. Xie, Q.H. Yang, Y.L. Liu, Dual band terahertz metamaterial absorber: design, fabrication, and characterization. *Appl. Phys. Lett.* **95**, 241111 (2009)
3. H. Tao, C.M. Bingham, D. Pilon, K.B. Fan, A.C. Strikwerda, D. Shrekenhamer, W.J. Padilla, X. Zhang, R.D. Averitt, A dual band terahertz metamaterial absorber. *J. Phys. D Appl. Phys.* **43**(22), 225102 (2010)
4. W.J. Padilla, A.J. Taylor, C. Highstrete, M. Lee, R.D. Averitt, Dynamical electric and magnetic metamaterial response at terahertz frequencies. *Phys. Rev. Lett.* **96**, 107401 (2006)
5. R. Parvaz, H. Karami, Far-infrared multi-resonant graphene-based metamaterial absorber. *Opt. Commun.* **396**, 267–274 (2017)
6. L. Wang, S.J. Ge, W. Hu, M.Y. Nakajima, Q. Lu, Graphene-assisted high efficiency liquid crystal tunable terahertz metamaterial absorber. *Opt. Express* **25**, 23873–23879 (2017)

7. B.Z. Ferdows, N.M. Mohammad, H. Samaneh, M. Mahshid, S.A. Afsaneh, Cross-slot nano-antenna with graphene coat for bio-sensing application. *Opt. Commun.* **371**, 34–39 (2016)
8. J. Linder, K. Halterman, Graphene-based extremely wide-angle tunable metamaterial absorber. *Sci. Rep.* **6**, 31225 (2016)
9. Y.T. Zhao, W.U. Bian, B.J. Huang, Q. Cheng, Switchable broadband terahertz absorber/reflector enabled by hybrid graphene-gold metasurface. *Opt. Express* **7**, 7161 (2017)
10. M. Cao, T. Wang, H. Zhang, Y. Zhang, Tunable electromagnetically induced absorption based on graphene. *Opt. Commun.* **413**, 73–79 (2018)
11. M. Nan, S. Shu, D. Hong, D. Shao, H. Qiong, Z. Lei, Hybridization-induced broadband terahertz wave absorption with graphene metasurfaces. *Opt. Express* **9**, 11728 (2018)
12. Z. Qi, L. Pei, B. Li, C. Xin, L. Han, Multi-band terahertz absorber exploiting graphene metamaterial. *Opt. Mater. Express* **8**, 2928 (2018)
13. S. Lee, T.Q. Tran, H. Heo, M. Kim, S. Kim, A proposal of a perfect graphene absorber with enhanced design and fabrication tolerance. *Sci. Rep.* **7**, 4760 (2017)
14. G.W. Hanson, Dyadic Green's functions and guided surface waves for a surface conductivity model of graphene. *J. Appl. Phys.* **103**, 064302 (2008)
15. D.R. Smith, D.C. Vier, T. Koschny, C.M. Soukoulis, Electromagnetic parameter retrieval from inhomogeneous metamaterials. *Phys. Rev. E* **71**, 036617 (2005)

Publisher's Note Springer Nature remains neutral with regard to jurisdictional claims in published maps and institutional affiliations.